23. Cheng, X. & Kaplan, L. A. Improved analysis of dissolved carbohydrates in stream water with HPLC-PAD. *Anal. Chem.* **73,** 458–461 (2001).
24. Newbold, J. D., Elwood, J. W., O'Neill, R. V. & Van Winkle, W. Measuring nutrient spiraling in streams. *Can. J. Fish. Aquat. Sci.* **38,** 860–863 (1981).

Supplementary Information accompanies the paper on **www.nature.com/nature**.

Acknowledgements We thank T. Georgian for insights regarding experimental design and the influence of biofilms on particle deposition; S. Roberts, M. Gentile and X. Cheng for technical assistance; K. Czymmek for CLSM support; and A. I. Packman, R. Sommaruga, G. Singer and J. Blaine for critically reading the manuscript. This work was supported by grants from the Austrian FWF (T.J.B.), the US NSF (L.A.K. and J.D.N.) and the Pennswood Fund for Environmental Research (L.A.K. and J.D.N.).

Competing interests statement The authors declare that they have no competing financial interests.

Correspondence and requests for materials should be addressed to T.J.B. (tomba@pflaphy.pph.univie.ac.at).

Balanced inhibition underlies tuning and sharpens spike timing in auditory cortex

Michael Wehr & Anthony M. Zador

Cold Spring Harbor Laboratory, 1 Bungtown Road, Cold Spring Harbor, New York 11724, USA

Neurons in the primary auditory cortex are tuned to the intensity and specific frequencies of sounds, but the synaptic mechanisms underlying this tuning remain uncertain. Inhibition seems to have a functional role in the formation of cortical receptive fields, because stimuli often suppress similar or neighbouring responses[1–3], and pharmacological blockade of inhibition broadens tuning curves[4,5]. Here we use whole-cell recordings *in vivo* to disentangle the roles of excitatory and inhibitory activity in the tone-evoked responses of single neurons in the auditory cortex. The excitatory and inhibitory receptive fields cover almost exactly the same areas, in contrast to the predictions of classical lateral inhibition models. Thus, although inhibition is typically as strong as excitation, it is not necessary to establish tuning, even in the receptive field surround. However, inhibition and excitation occurred in a precise and stereotyped temporal sequence: an initial barrage of excitatory input was rapidly quenched by inhibition, truncating the spiking response within a few (1–4) milliseconds. Balanced inhibition might thus serve to increase the temporal precision[6] and thereby reduce the randomness of cortical operation, rather than to increase noise as has been proposed previously[7].

Receptive fields are shaped by the interaction of excitation and inhibition. In the auditory cortex, indirect measurements of this interaction by extracellular methods[1–5] have suggested that it follows a classic organization—lateral inhibition—in which stimulation in the receptive field centre elicits excitation, and stimulation in the surround elicits inhibition[8]. Here we have used *in vivo* whole-cell patch-clamp methods to test that model directly by measuring synaptic inputs evoked by pure tones in rat auditory cortical neurons[9] (Fig. 1). For a subset of neurons (31/62), we improved the isolation of synaptic conductances by blocking action potentials with the fast sodium-channel blocker QX-314.

Tone-evoked synaptic conductance changes were large (Fig. 1c), comparable in magnitude to the largest conductance changes elicited by visual stimulation in area V1 neurons[10–12]. The true conductances were almost certainly higher than the values presented here, because voltage escape at the subsynaptic membrane due to electrotonic effects (space-clamp errors) causes an underestimation of synaptic conductances (see Supplementary Information). We

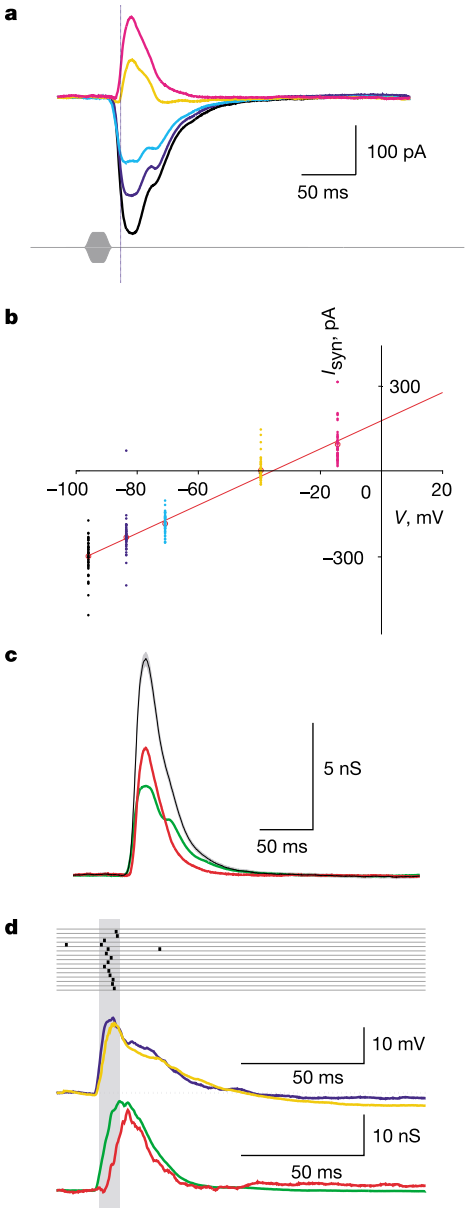

Figure 1 Tones evoked large transient excitatory and inhibitory conductances of comparable magnitudes. **a**, Synaptic currents evoked by a 25-ms tone pip at 1.2 kHz and 66 dB SPL at five holding potentials (48 repetitions). An offset response follows about 25 ms after the onset response. Spikes were blocked with QX-314. **b**, Instantaneous synaptic current-voltage (*I–V*) curve. Synaptic currents (coloured dots) are plotted against holding potential (colours as in **a**) for each of the 48 repetitions (means are indicated by red open circles) at the time of half-maximal synaptic conductance (33 ms from tone onset, indicated by the vertical blue line in **a**). The regression slope and *x*-intercept give, respectively, the instantaneous synaptic conductance (5.0 nS) and synaptic reversal potential (−36 mV). **c**, Continuous synaptic conductance (black line) with 95% regression confidence limits (shaded region), and its decomposition into excitatory (green) and inhibitory (red) conductances. Across all cells for which spikes were blocked, the maximal conductance evoked in each cell was 7.9 ± 9.7 nS, or 46 ± 54% of resting input conductance ($n = 31$ cells). **d**, In a different cell, for which spikes were not blocked, excitatory and inhibitory conductances (bottom, green and red traces) predicted the spikes (top, raster plot). The predicted (middle, blue trace, see Supplementary Methods) and actual (middle, orange trace) membrane potentials agreed closely.

decomposed the conductances into their underlying excitatory and inhibitory components[9,12,13] (see Supplementary Methods). The inhibitory conductance was typically as large as the excitatory conductance, which is consistent with the presence of shunting inhibition[10]. Each component followed approximately the same time course as the overall conductance waveform, showing a short-latency rise followed by a slower decay. Excitation evoked a transient spiking response (consisting of typically one or at most a few spikes; Fig. 1d) before being quenched by inhibition after a few milliseconds.

The total synaptic conductance was tuned for sound frequency (Fig. 2). The excitatory and inhibitory components were also tuned; moreover, they were co-tuned, showing approximately the same dependence on stimulus parameters in a given cell (Fig. 2a–d). Tuning of spiking responses was narrower than that of conductances or membrane potential (Fig. 3c), which is consistent with findings in auditory and other cortical regions[13–16]. Co-tuning differs from classical lateral inhibition[8], because excitation was at least as broadly tuned as inhibition, and sometimes more so; some surround stimuli elicited a purely excitatory response, whereas pure inhibition was never observed (Fig. 3a). The co-tuning we observed is therefore different from the organization described in some simple cells in primary visual cortex, in which excitation and inhibition can each be elicited in isolation within discrete spatial subregions[11,12], but is reminiscent of other simple cells in which excitation and inhibition are evoked together from each subregion[10].

Because inhibition had the same tuning as excitation, the tuning of the excitatory component alone would, in the absence of timing, be sufficient to establish a neuron's dependence on frequency. Although co-tuned inhibition sharpens tuning, this effect is equivalent to that of any untuned decrease in excitability, such as an increase in spike threshold. By means of this 'iceberg effect,' inhibition (shunting or otherwise) determines how much of the iceberg is suprathreshold but does not affect the shape of the iceberg itself (Fig. 3b); our results are therefore consistent with the finding that pharmacological blockade of inhibition broadens frequency tuning[4,5]. In this regard, frequency tuning in auditory cortex is similar to orientation tuning in some simple cells in primary visual cortex, which is sharpened by inhibition but which arises mainly through the convergence of thalamocortical inputs[17,18]. In contrast, orientation selectivity in other visual cortical neurons arises through a diversity of synaptic mechanisms[13] and can be influenced by recurrent cortical circuitry[19].

Two-tone suppression, in which one tone modifies (usually suppresses) the response to a later tone, has been interpreted as evidence of lateral inhibition in auditory cortical neurons[1,2,9,20]. Although our observations can explain how tuning is sharpened without lateral inhibition, they cannot by themselves account for two-tone suppression, which can last hundreds of milliseconds—longer than the inhibitory conductances we recorded (but see ref. 9). These suppressive effects might therefore be inherited from presynaptic neurons, or they might involve other mechanisms such as short-term synaptic plasticity[21,22].

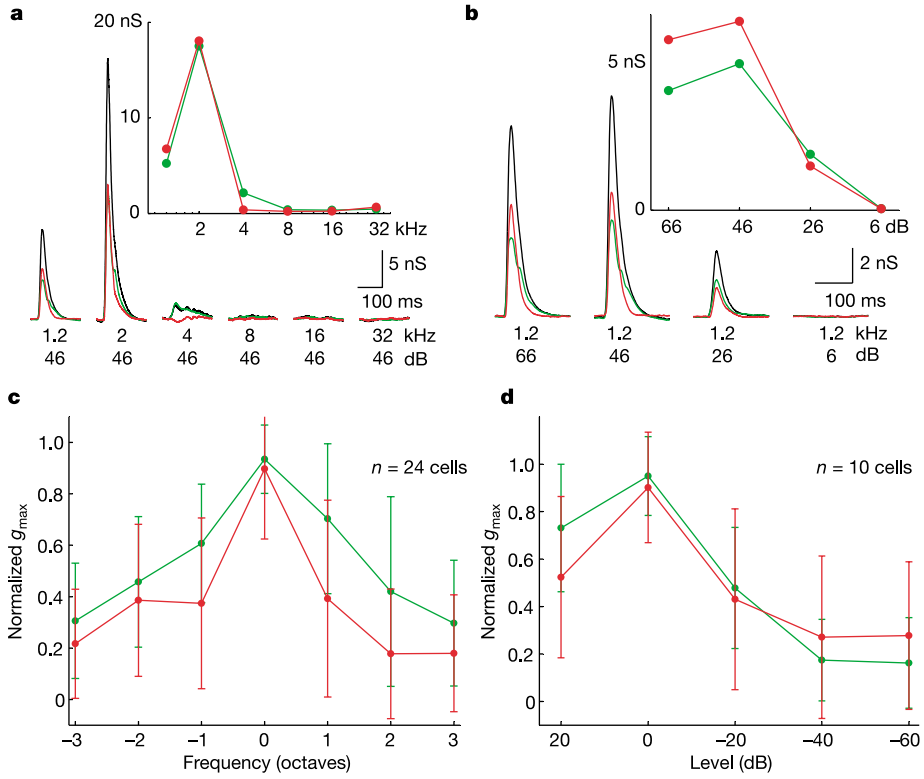

Figure 2 Excitatory, inhibitory, and total synaptic conductances were co-tuned for sound frequency and intensity. **a**, **b**, The total (black), excitatory (green) and inhibitory (red) synaptic conductances were all tuned for sound frequency (**a**) and intensity (**b**), matching the best frequency (2 kHz) and intensity (46 dB SPL) for this neuron (same cell as in Fig. 1a-c). Insets, Peak excitatory (green) and inhibitory (red) conductances showed similar tuning for frequency (**a**) and intensity (**b**). Error bars are obscured by the filled circles. For this neuron, as in most (29 of 31 cells), the stimulus that elicited maximal depolarization also elicited the maximal excitatory and total synaptic conductance. **c**, **d**, Co-tuning of normalized mean excitatory and inhibitory conductances for the population ($n = 229$ stimulus conditions in 31 cells with spikes blocked) against (**c**) ΔF and (**d**) ΔL, where ΔF is the frequency (in octaves) and ΔL is the intensity (in dB) relative to that which evoked maximal total synaptic conductance. For the population, excitation and inhibition were highly correlated (correlation coefficient $r = 0.80$). The ratio of inhibition to excitation tended to be fixed for a given neuron, but varied from one neuron to the next (this ratio was 0.74 ± 0.07 across cells, linear regression slope $\pm$95% confidence, but regression slopes across cells were significantly different from each other; ANCOVA, $P < 0.05$). Of the neurons tested, 70% (7 of 10) were tuned for sound intensity.

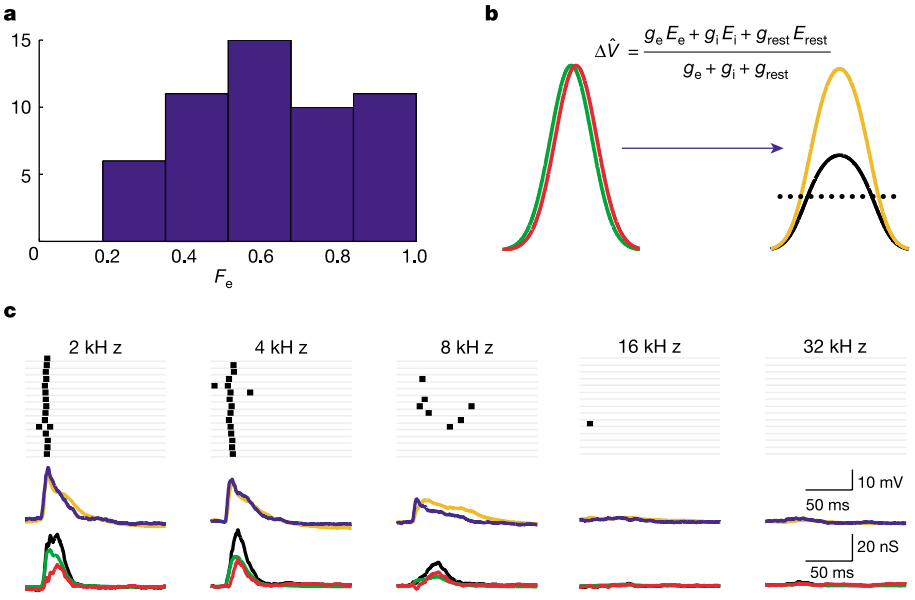

Figure 3 Co-tuned excitation and inhibition governs spiking. **a**, Distribution of the fraction of excitatory conductance $F_e = g_e/(g_e + g_i)$, where g_e and g_i are peak conductances (excitatory and inhibitory, respectively), across all stimuli (responses were included only if the total synaptic conductance was more than 1 nS); mean 0.61 ± 0.21 ($n = 53$ stimulus conditions in 11 cells). Note that pure inhibition was never observed ($F_e < 0.2$), whereas pure excitation was often observed ($F_e \approx 1$). **b**, Sharpening of tuning can arise from identical excitatory and inhibitory receptive fields. Idealized identical g_e (green) and g_i (red) tuning curves predict a depolarization tuning curve (black) that is sharpened in comparison with the depolarization produced by excitation alone (orange), especially when a spike initiation threshold (dotted horizontal line) is considered. **c**, For spiking cells, tuning of spikes was co-tuned with, and narrower than, subthreshold responses (same cell and format as in Fig. 1d). In all neurons for which tuning of both spikes and conductances could be assessed, the same stimulus elicited maximal spike count, peak excitatory conductance and peak inhibitory conductance ($n = 16$ cells). For this cell, root-mean-square error (see Supplementary Methods) between the predicted and actual V_m was 4.6 mV (population average 3.0 ± 2.6; $n = 21$).

Because inhibition did not seem to be essential to frequency tuning, we wondered whether it was involved in some form of gain control[23], perhaps resulting from the relatively loud (65 dB sound pressure level (SPL)) stimuli that we presented. We therefore tested a wide range of different stimulus intensities (5–65 dB SPL). However, we found that although total synaptic conductances were indeed tuned for sound intensity, the balance of excitation to inhibition remained fixed as intensity varied (Fig. 2b, d). Thus, co-tuning was a general feature of auditory cortical responses to simple tones across a wide range of frequencies and intensities.

Tuning for sound intensity (that is, a non-monotonic response to increasing intensity) has been proposed to result from lateral inhibition[24], which would predict that louder sounds should elicit stronger inhibition. Alternatively, intensity tuning might result from an increase in total input conductance[12], in which case louder sounds should elicit a larger total conductance change. However, neither prediction was satisfied; we found non-monotonicity in both excitatory and inhibitory synaptic conductances (Fig. 2b, d) underlying the response for all non-monotonic neurons, indicating that non-monotonicity was inherited from synaptic inputs[25]. These observations are consistent with the finding that non-monotonic cortical cells are not converted into monotonic cells by inhibitory blockade[5].

Because inhibition does not seem essential to either frequency or intensity tuning, what is its role? One key function of inhibition might be to sculpt the time course of tone-evoked responses. Excitation and inhibition appeared in a remarkably precise and stereotyped temporal sequence (Fig. 4): inhibition typically followed excitation after a brief delay (Fig. 4b). This sequence is consistent with that seen after electrical stimulation of the medial geniculate body[26]. In most cells this delay was independent of both frequency and intensity (Fig. 4c, f, g), indicating that relative timing did not usually have a function in frequency or intensity tuning. The delay was stereotyped in the range of 1–4 ms (Fig. 4e; the mean delay was 2.4 ± 3.6 ms, for $n = 50$ stimulus conditions in 17 cells) even though the latency to the onset of excitation varied, suggesting that inhibition was locked to the excitation rather than to the stimulus itself. Because the period between the onset of excitation and inhibition was short, only a brief window was available for integrating excitatory synaptic inputs. Spikes were elicited only during this brief excitatory window (Figs 1d and 3c). Thus, inhibition acts to enforce the transient[3,27], often binary[28], nature of stimulus-evoked responses in auditory cortex.

In a minority of cells (2 of 31, or 6%) the delay between excitation and inhibition was tuned for tone frequency (Fig. 4d). In these neurons the maximal depolarization corresponded not to the largest conductance but rather to the longest delay (and the least inhibition). Thus, in a fraction of neurons, timing might have a function in tuning. However, because we did not record spiking responses for these neurons, it is unclear whether these longer delays give rise to sustained firing here or in neurons driven by frequency-modulated sweeps, in which such long and stimulus-dependent delays have also been reported[9].

Although sensory stimuli elicit both excitation and inhibition in auditory and other sensory systems[9–14,29], the consistently short and stereotyped delay we observed between excitation and inhibition, and its relationship to transient spiking, have not previously been reported. In contrast, long and variable delays have been proposed to underlie sweep selectivity in auditory cortex[9]. This difference between short, sterotyped delays and long, variable delays might be due to the differences in stimuli (tones as opposed to sweeps), suggesting that excitatory–inhibitory delays might have different functional roles in shaping the responses to different classes of sounds. Similarly, excitation and inhibition in some simple cells of the primary visual cortex seem to have discrete subregions in space[11], yet are co-tuned for orientation[12].

A balance between excitation and inhibition has previously been proposed to account for the apparently random firing of cortical

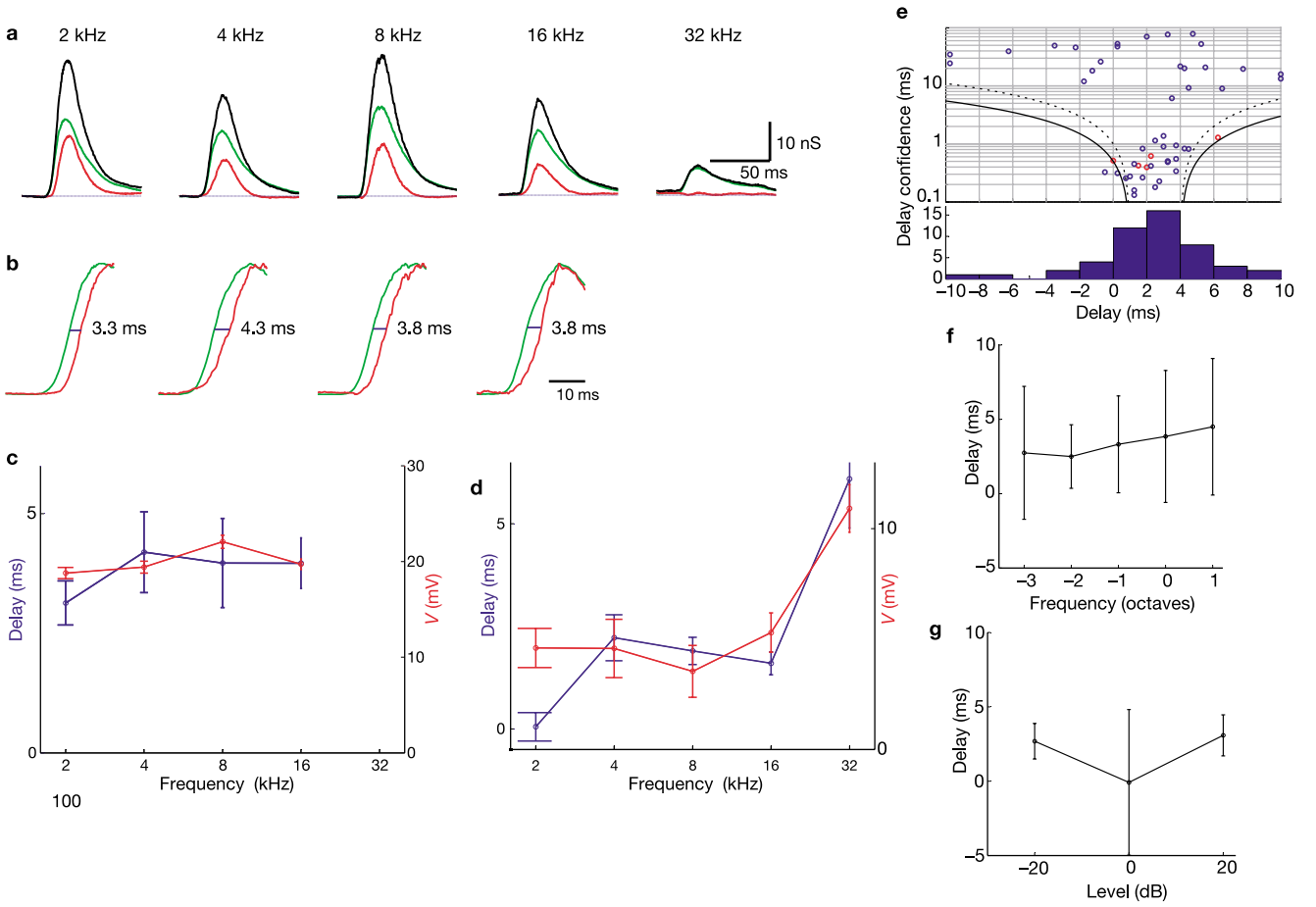

Figure 4 Excitatory conductance preceded inhibitory conductance by a brief delay. **a**, The excitatory conductance (green) led the inhibitory conductance (red) across frequencies (different neuron from those shown in Figs 1–3). **b**, Delays were extracted from normalized conductance waveforms at half maximal amplitude (excitation minus inhibition). **c**, Delays (blue circles, left ordinate) and peak $\Delta\hat{V}_m$ (red circles, right ordinate) for this cell, plotted as a function of frequency. Error bars are standard deviations obtained by bootstrap resampling. **d**, For a different cell, delay followed the same trend as peak $\Delta\hat{V}_m$ as a function of frequency: both were maximal at the best frequency (32 kHz) for this cell (symbols as in **c**). **e**, Bottom: distribution of delays across all cells and stimuli. The mean delay was 2.4 ± 3.6 ms ($n = 17$ cells). For normalization, responses were included only if both excitation and inhibition were more than 2 nS. Delays of more than 20 ms (corresponding to delays between onset and offset responses) were discarded. Top: for each response, delay is plotted against its confidence level (the standard deviation obtained by bootstrap resampling). Delays with strong confidence (that is, small values on the ordinate) tend to fall in the range 1–4 ms. All but two delays fall within two standard deviations (solid curve) of the range 1–4 ms (dotted line shows one standard deviation), as expected by chance. Responses from the delay-tuned cell in **d** are shown in red. **f**, **g**, Delay plotted against ΔF ($n = 13$ cells) (**f**) and ΔL ($n = 4$ cells) (**g**). Across the population, delay did not show a significant effect of either frequency or intensity (one-way ANOVA).

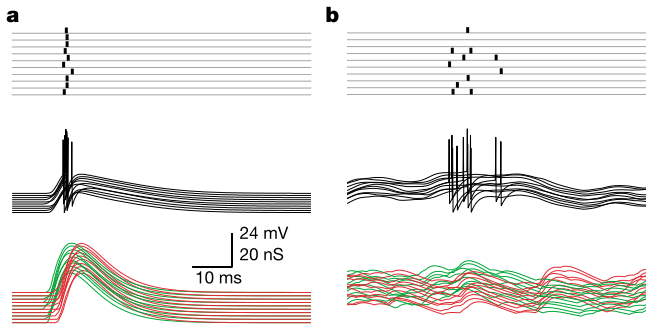

Figure 5 Simulation showing that excitation followed by balanced inhibition increases temporal precision, whereas excitation balanced on average by inhibition decreases temporal precision, using an integrate-and-fire model. **a**, Simulated synaptic input volleys had a mean inhibitory delay of 2.5 ms and a jitter of 1 ms standard deviation. From bottom to top: resulting excitatory (green) and inhibitory (red) synaptic conductances; resulting membrane potential (black lines); and output spike times (black vertical marks) for ten repeated trials. Time jitter in the output spike was 0.6 ms, indicating that inhibitory quenching increased temporal precision relative to the 1-ms input jitter. **b**, When excitatory and inhibitory synaptic inputs were instead balanced on average over a 100-ms window, again with 1 ms trial-to-trial jitter, firing was highly sensitive to input jitter. Time jitter in the output spike was 4.7 ms, indicating that balanced inhibition increased randomness. (Because inputs in **b** were spread out over a longer time window than in **a**, the number of inputs was increased from 20 to 56 to achieve the same mean spike count of 1.0 per trial.

neurons by producing large random fluctuations in the membrane potential[7]. In such models, however, it is only the average rate of excitatory and inhibitory postsynaptic potentials that is balanced; the individual events occur at random times, like raindrops. By contrast, the tight coordination we observed reflects a more precise control of cortical circuitry, unlikely to arise from random and independent synaptic activity arriving at a uniform rate[30]. Moreover, the rapid quenching of excitation by inhibition limits the window available for temporal summation, enabling neurons to behave as coincidence detectors and thereby increasing temporal precision[6].

We illustrate this distinction by using a simple integrate-and-fire model (Fig. 5). Balanced but delayed inhibition decreased the trial-to-trial jitter in output spike times compared with the jitter in the input spike times (from 1 ms to 0.6 ms; Fig. 5a), whereas excitation and inhibition that were balanced on average instead increased spike time jitter (from 1 ms to 4.7 ms; Fig. 5b). In both of these models, excitation and inhibition are balanced, but in a different sense: a continuing balance produces irregular firing (similar to responses observed in visual cortex, which motivate such models), whereas the transient and temporally offset balance we have observed produces highly transient spiking responses (Figs 1d and 3c), which is consistent with previous findings in auditory cortex[3,27,28]. Thus our data suggest that balanced inhibition can sharpen neural responses in time, reducing rather than increasing the randomness of cortical operation. □

Methods

We recorded from 62 cells in primary auditory cortex (all subpial depths) of anaesthetized (ketamine–medetomidine) rats aged 17–24 days after birth, using standard blind *in vivo* whole-cell methods. Pure tones had a duration of either 25 ms with a 5 ms 10–90% cosine-squared ramp, or 70 ms with a 20 ms ramp, and were delivered free-field at a rate of 1–2 per second using a calibrated electrostatic speaker in a double-walled sound booth. Total synaptic conductance, corrected for series resistance, was computed assuming an isopotential neuron (see Supplementary Methods for further details).

Received 17 March; accepted 10 October 2003; doi:10.1038/nature02116.

1. Shamma, S. A. & Symmes, D. Patterns of inhibition in auditory cortical cells in awake squirrel monkeys. *Hear. Res.* **19,** 1–13 (1985).
2. Calford, M. B. & Semple, M. N. Monaural inhibition in cat auditory cortex. *J. Neurophysiol.* **73,** 1876–1891 (1995).
3. Sutter, M. L., Schreiner, C. E., McLean, M., O'Connor, K. N. & Loftus, W. C. Organization of inhibitory frequency receptive fields in cat primary auditory cortex. *J. Neurophysiol.* **82,** 2358–2371 (1999).
4. Chen, Q. C. & Jen, P. H. Bicuculline application affects discharge patterns, rate-intensity functions, and frequency tuning characteristics of bat auditory cortical neurons. *Hear. Res.* **150,** 161–174 (2000).
5. Wang, J., McFadden, S. L., Caspary, D. & Salvi, R. Gamma-aminobutyric acid circuits shape response properties of auditory cortex neurons. *Brain Res.* **944,** 219–231 (2002).
6. Pouille, F. & Scanziani, M. Enforcement of temporal fidelity in pyramidal cells by somatic feed-forward inhibition. *Science* **293,** 1159–1163 (2001).
7. Shadlen, M. N. & Newsome, W. T. The variable discharge of cortical neurons: implications for connectivity, computation, and information coding. *J. Neurosci.* **18,** 3870–3896 (1998).
8. Hartline, H. K., Wagner, H. G. & Ratcliff, F. Inhibition in the eye of *Limulus*. *J. Gen. Physiol.* **39,** 651–673 (1956).
9. Zhang, L. I., Tan, A. Y., Schreiner, C. E. & Merzenich, M. M. Topography and synaptic shaping of direction selectivity in primary auditory cortex. *Nature* **424,** 201–205 (2003).
10. Borg-Graham, L. J., Monier, C. & Fregnac, Y. Visual input evokes transient and strong shunting inhibition in visual cortical neurons. *Nature* **393,** 369–373 (1998).
11. Hirsch, J. A., Alonso, J. M., Reid, R. C. & Martinez, L. M. Synaptic integration in striate cortical simple cells. *J. Neurosci.* **18,** 9517–9528 (1998).
12. Anderson, J. S., Carandini, M. & Ferster, D. Orientation tuning of input conductance, excitation, and inhibition in cat primary visual cortex. *J. Neurophysiol.* **84,** 909–926 (2000).
13. Monier, C., Chavane, F., Baudot, P., Graham, L. J. & Fregnac, Y. Orientation and direction selectivity of synaptic inputs in visual cortical neurons: a diversity of combinations produces spike tuning. *Neuron* **37,** 663–680 (2003).
14. Moore, C. I. & Nelson, S. B. Spatio-temporal subthreshold receptive fields in the vibrissa representation of rat primary somatosensory cortex. *J. Neurophysiol.* **80,** 2882–2892 (1998).
15. Carandini, M. & Ferster, D. Membrane potential and firing rate in cat primary visual cortex. *J. Neurosci.* **20,** 470–484 (2000).
16. Ojima, H. & Murakami, K. Intracellular characterization of suppressive responses in supragranular pyramidal neurons of cat primary auditory cortex *in vivo*. *Cereb. Cortex* **12,** 1079–1091 (2002).
17. Chung, S. & Ferster, D. Strength and orientation tuning of the thalamic input to simple cells revealed by electrically evoked cortical suppression. *Neuron* **20,** 1177–1189 (1998).
18. Miller, L. M., Escabi, M. A., Read, H. L. & Schreiner, C. E. Functional convergence of response properties in the auditory thalamocortical system. *Neuron* **32,** 151–160 (2001).
19. Schummers, J., Marino, J. & Sur, M. Synaptic integration by V1 neurons depends on location within the orientation map. *Neuron* **36,** 969–978 (2002).
20. Phillips, D. P. & Cynader, M. S. Some neural mechanisms in the cat's auditory cortex underlying sensitivity to combined tone and wide-spectrum noise stimuli. *Hear. Res.* **18,** 87–102 (1985).
21. Volkov, I. O. & Galazyuk, A. V. Peculiarities of inhibition in cat auditory cortex neurons evoked by tonal stimuli of various durations. *Exp. Brain Res.* **91,** 115–120 (1992).
22. Chung, S., Li, X. & Nelson, S. Short-term depression at thalamocortical synapses contributes to rapid adaptation of cortical sensory responses *in vivo*. *Neuron* **34,** 437–446 (2002).
23. Chance, F. S., Abbott, L. F. & Reyes, A. D. Gain modulation from background synaptic input. *Neuron* **35,** 773–782 (2002).
24. Phillips, D. P. Effect of tone-pulse rise time on rate-level functions of cat auditory cortex neurons: excitatory and inhibitory processes shaping responses to tone onset. *J. Neurophysiol.* **59,** 1524–1539 (1988).
25. De Ribaupierre, F., Goldstein, M. H. Jr & Yeni-Komshian, G. Intracellular study of the cat's primary auditory cortex. *Brain Res.* **48,** 185–204 (1972).
26. Mitani, A. & Shimokouchi, M. Neuronal connections in the primary auditory cortex: an electrophysiological study in the cat. *J. Comp. Neurol.* **235,** 417–429 (1985).
27. Brugge, J. F., Dubrovsky, N. A., Aitkin, L. M. & Anderson, D. J. Sensitivity of single neurons in auditory cortex of cat to binaural tonal stimulation; effects of varying interaural time and intensity. *J. Neurophysiol.* **32,** 1005–1024 (1969).
28. DeWeese, M. R., Wehr, M. & Zador, A. M. Binary spiking in auditory cortex. *J. Neurosci.* **23,** 7940–7949 (2003).
29. Covey, E., Kauer, J. A. & Casseday, J. H. Whole-cell patch-clamp recording reveals subthreshold sound-evoked postsynaptic currents in the inferior colliculus of awake bats. *J. Neurosci.* **16,** 3009–3018 (1996).
30. Stevens, C. F. & Zador, A. M. Input synchrony and the irregular firing of cortical neurons. *Nature Neurosci.* **1,** 210–217 (1998).

Supplementary Information accompanies this paper on **www.nature.com/nature**.

Acknowledgements We thank K. Miller, L. Miller, M. Kvale, Z. Mainen, M. DeWeese and M. Sutter for comments on an earlier version of this manuscript. This work has been supported by grants to A.M.Z. from the Packard Foundation, the Sloan Foundation, the NIH and the Mathers Foundation.

Competing interests statement The authors declare that they have no competing financial interests.

Correspondence and requests for materials should be addressed to A.M.Z. (zador@cshl.edu)

An ancient role for nuclear β-catenin in the evolution of axial polarity and germ layer segregation

Athula H. Wikramanayake[1], Melanie Hong[1,2], Patricia N. Lee[2], Kevin Pang[2], Christine A. Byrum[1], Joanna M. Bince[1], Ronghui Xu[1] & Mark Q. Martindale[2]

[1]*Department of Zoology, University of Hawaii at Manoa, 2538 McCarthy Mall, Honolulu 96822, Hawaii*
[2]*Kewalo Marine Lab/Pacific Biomedical Research Center, University of Hawaii, 41 Ahui Street, Honolulu 96813, Hawaii*

The human oncogene β-catenin is a bifunctional protein with critical roles in both cell adhesion and transcriptional regulation in the Wnt pathway[1–3]. Wnt/β-catenin signalling has been implicated in developmental processes as diverse as elaboration of embryonic polarity[2–6], formation of germ layers[4–8], neural patterning, spindle orientation and gap junction communication[2], but the ancestral function of β-catenin remains unclear. In many animal embryos, activation of β-catenin signalling occurs in blastomeres that mark the site of gastrulation and endomesoderm formation[5–10], raising the possibility that asymmetric activation of β-catenin signalling specified embryonic polarity and segregated germ layers in the common ancestor of bilaterally symmetrical animals. To test whether nuclear translocation of β-catenin is involved in axial identity and/or germ layer formation in 'pre-bilaterians', we examined the *in vivo* distribution, stability and function of β-catenin protein in embryos of the sea anemone *Nematostella vectensis* (Cnidaria, Anthozoa). Here we